JOURNAL OF BACTERIOLOGY, Jan. 1987, p. 42–52
0021-9193/87/010042-11$02.00/0

Vol. 169, No. 1

Genetic and Molecular Characterization of the Genes Involved in Short-Chain Fatty Acid Degradation in *Escherichia coli*: the *ato* System

LAUREN SALLUS JENKINS†* AND WILLIAM D. NUNN‡

Department of Molecular Biology and Biochemistry, University of California at Irvine, Irvine, California 92717

Received 2 June 1986/Accepted 2 October 1986

The structural organization and regulation of the genes involved in short-chain fatty acid degradation in *Escherichia coli*, referred to as the *ato* system, have been studied by a combination of classic genetic and recombinant DNA techniques. A plasmid containing a 6.2-kilobase region of the *E. coli* chromosome was able to complement mutations in the *ato* structural genes, *atoA* (acetyl-coenzyme A [CoA]:acetoacetyl [AA]-CoA transferase) and *atoB* (thiolase II), as well as mutations in the *ato* regulatory locus, *atoC*. Complementation studies performed with mutants defective in acetyl-CoA:AA-CoA transferase suggest that two loci, *atoD* and *atoA*, are required for the expression of functional AA-CoA transferase. The *ato* gene products were identified by in vitro transcription and translation and maxicell analysis as proteins of 48, 26.5, 26, and 42 kilodaltons for *atoC*, *atoD*, *atoA*, and *atoB*, respectively. In vitro and insertional mutagenesis of the *ato* hybrid plasmid indicated that the *ato* structural genes were arranged as an operon, with the order of transcription *atoD-atoA-atoB*. Although transcribed in the same direction as the *atoDAB* operon, the *atoC* gene appeared to use a promoter which was distinct from that used by the *atoDAB* operon. A Δ*atoC* plasmid expressed the *atoD*, *atoA*, and *atoB* gene products only in strains containing a functional *atoC* gene. Although the exact mechanism of control was not evident from these studies, the data suggest that the *atoC* gene product is an activator which is required for the synthesis or activation of the *atoDAB*-encoded enzymes.

The four-carbon β-keto short-chain fatty acid (SCFA) acetoacetate (AA) can be used by wild-type *Escherichia coli* as a sole carbon and energy source (7, 16, 22). The degradation of AA to acetyl coenzyme A (acetyl-CoA) is a two-step reaction (Fig. 1). The activation of AA to acetoacetyl-CoA is catalyzed by acetyl-CoA:AA-CoA transferase and is followed by the subsequent cleavage of AA-CoA to acetyl-CoA by thiolase II. These enzymes are highly inducible in the presence of AA and are specific for SCFA substrates (22).

Earlier studies performed by Pauli and Overath identified the loci responsible for AA degradation as *atoA* (which encodes AA-CoA transferase) and *atoB* (which encodes thiolase II) (22). These structural genes are closely linked and are located at the min 47 region of the revised *E. coli* chromosomal map (22). Studies by Duncombe and Frerman (10) and Sramek and Frerman (30) demonstrated that AA-CoA transferase is a tetrameric protein with an $\alpha_2\beta_2$ composition (α subunit, M_r 26,000 [26K]; β subunit, 23K), and thiolase II is a tetrameric protein composed of four identical polypeptides of 42K. This latter work suggested that the subunits of AA-CoA transferase are probably encoded by two separate genes.

Although AA can be utilized by wild-type strains, the saturated SCFAs butyrate (BUT) and valerate (VAL) cannot directly serve as substrates for the ATO enzymes (16, 22). For BUT or VAL to be metabolized, the ATO enzymes are required as well as the fatty acid degradative enzymes encoded by the *fadE* and *fadB* structural genes (Fig. 1). Since expression of the *ato* and *fad* structural genes is not induced by saturated SCFAs, two mutations causing constitutive expression of the *ato* and *fad* structural genes are necessary for the metabolism of saturated SCFAs (22). Strains bearing a *fadR* mutation constitutively express the fatty acid degradative (*fad*) genes. *E. coli* strains bearing the *fadR* mutation can grow on medium-chain (C_7 to C_{11}) and long-chain (C_{12} to C_{18}) fatty acids but not on saturated SCFAs because these substrates cannot induce the ATO enzymes. Constitutive levels of the ATO enzymes result from a mutation in the regulatory gene, *atoC*, which also maps at min 47 (22). Mutants able to utilize butyrate (But^+) as a sole carbon source are readily selected by plating *fadR* strains on minimal medium containing BUT (22). Pauli and Overath (22) first showed that most But^+ mutants obtained in this way were constitutive for the ATO enzymes. The mutation causing constitutivity of the ATO enzymes has been termed *atoC* (Con). Merodiploid studies demonstrated that the *atoC* (Con) genotype was *trans*-dominant to the wild-type $atoC^+$ allele. From these studies Pauli and Overath suggested that *atoC* encodes an activator (22).

To determine whether AA-CoA transferase is encoded by two genes and to further characterize the *atoC* regulatory locus, mutants were isolated and characterized by genetic and biochemical analyses. To characterize the physical organization of the *ato* structural and regulatory genes, the *atoCAB* region has been cloned into a multicopy plasmid. The approximate location, orientation, and direction of transcription of the *ato* genes were determined by subcloning and transposon mutagenesis. The *ato*-encoded gene products were identified by maxicell analyses and in vitro transcription and translation analyses. To gain a better understanding of the regulation of the *ato* structural genes, we have isolated and examined a collection of *atoC* mutants.

* Corresponding author.
† Present address: Department of Genetics, Stanford University School of Medicine, Stanford, CA 94305.
‡ Deceased 1 July 1986.

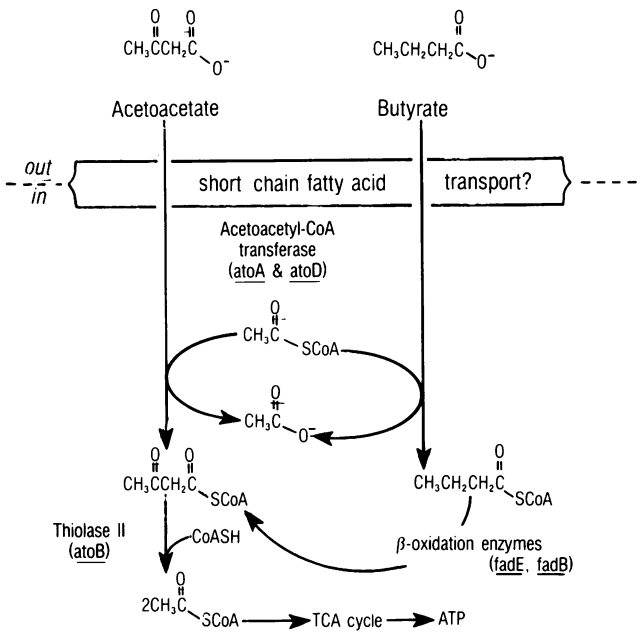

FIG. 1. Pathway of SCFA degradation. The principal enzymes are listed along with the respective structural genes of the *ato* and *fad* systems.

Characterization of these mutants supports the model that *atoC* encodes a positive regulatory element.

MATERIALS AND METHODS

Bacterial strains, plasmids, and growth conditions. The bacterial strains used in this study are derivatives of *E. coli* K-12 and are listed in Table 1. The plasmids used in this study are derivatives of pBR322 and are listed in Table 2.

The bacteria were routinely grown in Luria broth (LB) or tryptone broth (TB) and incubated in a New Brunswick Gyratory water bath shaker at 37°C. Minimal medium E (20) was used for both the complementation studies and enzyme assays, whereas sulfate-free M9 minimal medium (4) was used for the maxicell procedure. These minimal media were supplemented with carbon sources at the following final concentrations: acetate, 50 mM; AA, 10 mM; and sugars, 4 mg/ml. AA was prepared as a stock solution of 0.25 M, neutralized with NaOH, and added to liquid or solid media at a final concentration of 10 mM. The fatty acids 4-pentenoate (4P), decanoate, and oleate were suspended in 10% Brij 58, neutralized with KOH, and sterilized. 4P was added at a final concentration of 10 mM, and decanoate and oleate were added at final concentrations of 5 mM. Amino acids were added when necessary at a final concentration of 0.01%. Antibiotics were used at the following final concentrations; ampicillin, 100 μg/ml; kanamycin, 45 μg/ml; and tetracycline, 10 μg/ml. Carbon sources, supplements, and antibiotics were sterilized separately and added to culture media prior to inoculation. Solid minimal medium E supplemented with 10 mM AA was used to screen for growth on AA.

Strain constructions. (i) Construction of Tn*10* insertions near the *ato* region of the chromosome. Strains with transposon Tn*10* insertions near the *ato* region in the host chromosome, designated *zeh*::Tn*10* (strains LJ7, LJ9, and LJ300) were generated by transducing an *atoA* Tet^s host (K2006) with a phage φP1 *vir* Tn*10* pool (28) with selection for AA$^+$ Tet^r transductants. The location of the Tn*10* element was determined by transducing an *atoC* (Con), *atoB*, or *gyrA* host with phage stocks of each of the above mentioned *ato*-linked Tn*10* insertion mutants (strains LJ7, LJ9, and LJ300) and determining the frequency of cotransduction of the Tn*10* marker with the *atoC* (Con), *atoB*, and *gyrA*. The Tn*10* insertions in strains LJ7 and LJ9 were found to be between *ompC* and *atoC* and were 70 and 95% cotransducible with the *atoC* (Con) marker, respectively. Strain LJ300 resulted in a Tn*10* insertion between *atoB* and *gyrA*, with a cotransduction frequency of 85% with respect to *atoB*.

(ii) Construction of the Δ*ato* null host LJ111. The Δ(*atoCDAB*) mutant was obtained by first transducing strain LE392 with phage φP1 *vir* grown on LJ9 (*zeh-9*::Tn*10*) and selecting for Tet^r colonies. Next, a disruption in the *ato* region (e.g., deletion, inversion, or rearrangement) was generated by plating these Tet^r AA$^+$ colonies on medium that selects directly for Tet^s colonies (24). The Tet^s colonies were screened for growth on AA to determine whether the excision resulted in the deletion or inversion of the *ato* region. The deletions or inversions in the AA$^-$ Tet^s colonies were mapped by transducing these isolates with phage φP1 *vir* grown on LJ26 (*zeh-7*::Tn*10 atoA*) and LJ29 (*zeh-7*::Tn*10 atoB*) and screening the Tet^r transductants for growth on

TABLE 1. Bacterial strains

Strain	Relevant genotype[a]	Reference or source
LE392	*metB hsdR galK trpR lacY*	Cold Spring Harbor Laboratory
LS3010	*fadR*	R. Simons (28)
LS5218	*fadR atoC2*(Con)	S. Spratt (30)
NK5304	*srlA*::Tn*10 recA*	N. Kleckner
MC4100	*araD139* Δ(*argF-lac*)*U169*	M. Casadaban
MC4100rA	MC4100 *srlA*::Tn*10 recA*	φP1 NK5304 × MC4100
K2006	*his fadR16 fadA30 atoC49*(Con) *atoA28*	P. Overath (22)
K2006rA	K2006 *srlA*::Tn*10 recA*	φP1 NK5304 × K2006
K2008	*his fadR16 fadA30 atoC49*(Con) *ato(AB)37*	P. Overath (22)
2008rA	K2008 *srlA*::Tn*10 recA*	φP1 NK5304 × K2008
K2009	*his fadR16 fadA30 atoC49*(Con) *atoB58*	P. Overath (22)
K2009rA	K2009 *srlA*::Tn*10 recA*	φP1 NK5304 × K2009
LJ7	LE392 *zeh-7*::Tn*10*	This study
LJ9	LE392 *zeh-9*::Tn*10*	This study
LJ300	LE392 *zeh-300*::Tn*10*	This study
LJ26	K2006 *zeh-7*::Tn*10*	This study
LJ29	K2009 *zeh-7*::Tn*10*	This study
LJ14	*atoC2*(Con) *atoA14*	This study
LJ14rA	LJ14*srlA*::Tn*10 recA*	φP1 NK5304 × LJ14
LJ32	*atoC2*(Con) *atoD32*	This study
LJ32rA	LJ32 *srlA*::Tn*10 recA*	φP1 NK5304 × LJ32
LJ31	LS5218 *atoC31 atoA*$^+$ *atoB*$^+$	This study
LJ31rA	LJ31 *srlA*::Tn*10 recA*	This study
LJ61	LS5218 *atoC61 atoA*$^+$ *atoB*$^+$	This study
LJ61rA	LJ61 *srlA*::Tn*10 recA*	This study
LJ111	LE392 Δ(*atoCDAB*)	This study
LJ112	LJ111 *srlA*::Tn*10 recA*	φP1 NK5304 × LJ111

[a] The nomenclature for genetic symbols follows that of Bachman and Low (3), and the nomenclature for transpositional insertions follows that of Kleckner et al. (15).

TABLE 2. Plasmids

Plasmid	Relevant genotype of properties[a]	Reference or source
pBR322	Ap^r Tc^r	6
pKO9	Ap^r $\Delta galK$	C. Adams (1)
pLJ10	*atoCDAB*$^+$ Ap^r	This study
pLJ11	*atoCDA*$^+$ $\Delta atoB$ Ap^r	This study
pLJ12	*atoCDA*$^+$ $\Delta atoB$ Ap^r	This study
pLJ13	*atoCD*$^+$ $\Delta atoAB$ Ap^r	This study
pLJ14	*atoCD*$^+$ $\Delta atoA$ *atoB*$^+$ Ap^r	This study
pLJ15	$\Delta atoCDA$ *atoB*$^+$ Ap^r	This study
pLJ16	$\Delta atoC$ *atoDAB*$^+$ Ap^r	This study
pLJ17	Ap^r AA^- Φ(*atoD-galK*)	This study
pLJ18	$\Delta atoC$ Ap^r	This study
pLJ19	$\Delta atoC$ Ap^r	This study
pMKB1	*atoB1*::mk Ap^r Km^r	This study
pMKB2	*atoB2*::mk Ap^r Km^r	This study
pMKB3	*atoB3*::mk Ap^r Km^r	This study
pMKB4	*atoB4*::mk Ap^r Km^r	This study
pMKA	$\Delta atoA$::mk Ap^r Km^r	This study
pMKC1	*atoC1*::mk Ap^r Km^r	This study
pMKC2	*atoC2*::mk Ap^r Km^r	This study
pMKC3	*atoC3*::mk Ap^r Km^r	This study

[a] mk, Mini-Kan^r insertion.

AA. Infection of strain LJ111 with either the *atoA* or *atoB* phage stocks resulted in no AA^+ transductants (>500 colonies scored). This lack of AA^+ recombinants suggests that a deletion rather than an inversion has occurred within the *ato* region. Since the Tn*10* marker is to the left of the *atoC* gene, the deletion should extend through the *atoC* region.

(iii) Construction of the *atoC*, *atoD*, and *atoA* mutants. Strains unable to use AA as a sole carbon source were obtained by plating the *atoC* (Con) *fadR* strain LS5218 onto minimal medium containing 10 mM 4P and 5 mM decanoate. Decanoate was used as the carbon source to maintain the *fadR* genotype. The $4P^r$ colonies were isolated and screened for lack of growth on AA. Mutations resulting in the AA^- $4P^r$ phenotype were localized to the *ato* region by transducing these isolates with phage ϕP1 *vir* grown on LJ9 (*zeh-9*::Tn*10*). AA-CoA transferase and thiolase enzyme assays were performed on the *ato* mutants to determine the site of the mutation. Strains LJ14 and LJ32 had constitutive thiolase activity but lacked AA-CoA transferase activity, indicating that they harbored a mutation in the gene(s) coding for the subunits of AA-CoA transferase. Strains LJ31 and LJ61 had a pleiotropic loss of AA-CoA transferase and thiolase activities, suggesting a mutation in the putative activator encoded by *atoC*.

Isolation and manipulation of DNA. Large-scale isolation and purification of plasmid DNA was done by the cleared lysate-polyethylene glycol precipitation method of Humphreys et al. (13). Supercoiled plasmid DNA was further isolated by centrifugation in a CsCl density gradient containing ethidium bromide (24). Small-scale plasmid isolation was performed as described by Ish-Horowicz and Burke (14). Digestion of DNA with restriction enzymes was generally carried out as described by the vendor (Bethesda Research Laboratories) or Maniatis et al. (19). Restriction fragments were analyzed by electrophoresis in agarose slab gels prepared in TEA buffer (50 mM Tris, 20 mM sodium acetate, 2 mM disodium EDTA [pH 8.05]) (12).

E. coli cells were prepared for transformation by the procedure described by Dagert and Ehrlich (8). AA^+ transformants were screened on solid minimal medium E supplemented with 10 mM AA and the appropriate antibiotic. AA^+ transformants appeared in 2 to 3 days at 37°C.

The *E. coli* genomic DNA library used to isolate the AA^+ clone pLJ10 was constructed by C. DiRusso (9). *E. coli* chromosomal DNA was partially digested with *Sau*3A and size selected for fragments between 5 and 20 kilobases (kb). The size-fractionated chromosomal DNA was ligated into the *Bam*HI site of pBR322, and this ligation mix was transformed into LE392. Plasmids were extracted from a pool of 4,000 Amp^r colonies, of which at least 75% were Tet^s, indicating that the plasmids contained an insert in the Tet^r gene. This plasmid pool was used to isolate the AA^+ clone designated pLJ10.

Construction of pLJ10 derivative plasmids. Derivatives of plasmid pLJ10 (pLJ11, pLJ12, pLJ13, pLJ14, pLJ15, and pLJ16) were constructed by the following method. pLJ10 was individually digested with the appropriate restriction enzyme and then ligated in vitro with T4 ligase at 4°C in 66 mM Tris hydrochloride (pH 7.6)–6.6 mM $MgCl_2$–10 mM dithiothreitol–0.5 mM ATP for 16 to 24 h (19). Plasmid pLJ17 was constructed by inserting the 1.2- to 2.6-kb *ato* region from pLJ10 into the *Bam*HI site of pKO9.

pLJ18 was constructed by complete digestion of pLJ12 with the endonucleases *Bam*HI and *Bgl*II and isolating a 5.5-kb region that contains the 0.0- to 1.2-kb *ato* region along with the entire pBR322 fragment. This fragment was ligated in vitro with T4 ligase. pLJ19 was constructed by restricting pLJ10 with *Eco*RI to completion and isolating a 5.5-kb fragment. This fragment contained most of the pBR322 sequences along with the 0.0- to 1.5-kb region of the *ato* insert. This fragment was ligated in vitro with T4 ligase. These ligation mixtures were used to transform the putative *atoC* strains LJ31 and LJ61 to Amp^r Plasmid DNA was isolated from the resulting transformants, digested with the enzyme previously used, and analyzed as described above.

Preparation of cell extracts and enzyme assays. The bacteria were grown in induced conditions to mid-exponential phase in 10 ml of TB medium supplemented with 10 mM AA or in minimal medium E supplemented with 25 mM succinate, 10 mM AA, 0.1% Casamino Acids (Difco Laboratories), 0.01% L-tryptophan, and the appropriate antibiotics and amino acids. For cultures grown in uninduced conditions, the 10 mM AA was omitted from the culture medium. The cells were harvested and washed first in medium E and then in 10 mM KPO_4. The washed cells were then either stored at −20°C overnight or directly lysed with glass beads (450 to 500 μm diameter; Sigma Chemical Co.) in 300 μl of 10 mM KPO_4 buffer plus 0.1 mM phenylmethylsulfonyl fluoride. The protein content of the extracts was determined by the procedure of Lowry et al. (17) with bovine serum albumin as the standard.

AA-CoA transferase was assayed as previously described by Sramek and Frerman (31) with the following modifications. AA-CoA transferase activity was measured in the forward direction by monitoring the increase in A_{303} due to the formation of the enolate form of AA-CoA in the presence of $MgCl_2$. The enolate form of AA-CoA absorbs at 303 nm with an extinction coefficient of $E_{303} = 1.69 \times 10^2$ M. Incubation mixtures contained 67 mM Tris hydrochloride (pH 8.1), 5 mM $MgCl_2$, 0.2 mM acetyl-CoA, and 10 mM AA in a final volume of 300 μl. The reaction was initiated by addition of the acetyl-CoA substrate. Thiolase enzyme activity was measured as described by Spratt et al. (29). Enzyme reactions was monitored in a Beckman recording spectrophotometer at room temperature. All values are the average of at least three independent determinations.

TABLE 3. AA-CoA transferase and thiolase enzyme activities in *ato* mutants

Strain	Induction[a]	Sp act (nmol/min per mg of protein)[b]	
		AA-CoA transferase	Thiolase
LS5218	−	318	527
LJ14	−	0	431
	+	0	ND
LJ32	−	0	391
	+	0	ND
LJ31[c]	−	0	10
	+	0	11
LJ61[c]	−	0	9
	+	0	8

[a] Symbols: −, minimal medium supplemented with 25 mM succinate, 0.1% Casamino Acids, and 0.01% tryptophan; +, minimal medium supplemented with the above plus 10 mM AA.

[b] A measurement of zero implies activity of <0.1. ND, Not determined.

[c] Strains are *fadR fadA*$^+$, which accounts for the low constitutive thiolase levels observed in LJ31 and LJ61.

Protein identification. Plasmid-encoded proteins were labeled with [^{35}S]methionine either in vivo, by the procedure of Sancar et al. (26) and the modifications of Black et al. (5), or in vitro with the Amersham in vitro transcription-translation procedure.

Radioactively labeled proteins were analyzed by 9 or 12% sodium dodecyl sulfate (SDS)-polyacrylamide gel electrophoresis with appropriate molecular weight standards provided by BioRad Laboratories. Two-dimensional SDS-polyacrylamide gels were prepared as described by O'Farrell (21) with the modifications of Black et al. (5).

Insertional mutagenesis of pLJ10. Polar insertions within the 6.2-kb *ato* region of pLJ10 were generated by the procedure of Way et al. (35). Phage λNK1105 (kindly provided by N. Kleckner) contains a 1.67-kb mini-Kan^r insert flanked by deleted IS*10* elements. The *tetA* gene, which provides the transposase function, lies outside the insertional element. This construct results in optimal transposition frequencies and very stable insertions in the gene of interest. Plasmids that contained mini-Kan^r insertions within pLJ10 were generated by the techniques of Spratt et al. (29). Cultures of MC4100 *recA* harboring plasmid pLJ10 were grown to late exponential phase in TB broth supplemented with 10 mM $MgSO_4$, 0.2% maltose, and 100 μg of ampicillin per ml. Cells were washed in M9 and suspended in 10 mM $MgSO_4$ followed by infection with phage λNK1105 at a multiplicity of 1 phage per cell. After incubation for 30 min at 30°C, 1.0 ml of LB was added to the infected cells, which were grown at 30°C for 1 h to allow phenotypic expression. The cells were washed, suspended in M9, and spread on LB plates containing kanamycin and ampicillin to select for mini-Kan^r transpositional events and to maintain plasmid selection. Kan^r Amp^r colonies were pooled and diluted in 500 ml of LB containing kanamycin and ampicillin and incubated for 16 h at 37°C. The plasmid DNA was isolated by the small-scale technique (14) and used to transform the Δ(*atoCDAB*) Kan^s Amp^s host (strain LJ112) to Kan^r. All Kan^r Amp^r transformants were screened for their ability to utilize AA as a sole carbon source. The plasmids from the resulting AA$^-$ transformants (designated pMK) were isolated and transformed separately into various *ato* mutant strains (strains LJ32, LJ14, LJ112, K2006, and K2009) and screened for growth on AA. This 1.67-kb insertion element is flanked by *Bam*HI sites and contains unique *Hin*dIII and *Sma*I sites. These restriction sites, as well as various other restriction sites, were used to localize the site of insertion within pLJ10. The proteins encoded by the various pMK isolates were determined by maxicell procedure or in vitro transcription-translation analysis and SDS gel electrophoresis.

In vitro construction of the mini-Kan^r insert within pLJ10 was generated by first isolating the 1.67-kb mini-Kan^r insert via a *Bam*HI digest of pMKB1. The *Bam*HI ends of the 1.67-kb insert were filled with deoxynucleotide triphosphates with the Klenow fragment of DNA polymerase I in a reaction mixture containing 5 mM deoxynucleotide triphosphates and incubated at room temperature for 1 h. The blunt-ended mini-Kan^r region was inserted into the *Hpa*I site of pLJ14, yielding plasmid pMKA.

Chemicals. Antibiotics and other chemicals were obtained from Sigma Chemical Co. Restriction endonucleases, T4 DNA ligase, the large Klenow fragment of DNA polymerase I, and bacterial alkaline phosphotase were obtained from Bethesda Research Laboratories or Boehringer Mannheim. Acrylamide, bisacrylamide, TEMED, ammonium persulfate, and CsCl were obtained from Bethesda Research Laboratories (ultrapure). Ampholytes were obtained from Bio-Rad. All other chemicals were obtained from standard suppliers and were of reagent grade.

RESULTS

Isolation of *ato* mutants. The SCFA analog 4P was used to generate mutations in the gene(s) which encodes AA-CoA transferase (i.e., *atoA*) and in the *atoC* loci of the host chromosome. Previous investigators have shown that 4P inhibits fatty acid oxidation in bacteria and higher eucaryotes (11, 27). Salanitro and Wegener (25) showed that 4P selectively inhibits growth of *atoC*(Con) strains, which constitutively express the ATO enzymes, but not *ato*$^+$ strains, which express these enzymes only after induction. Therefore, *atoC*(Con) strains with constitutive levels of AA-CoA transferase are inhibited by 4P (i.e., 4P^s), whereas *atoC*(Con) strains harboring a defect in this enzyme are 4 P^r. These studies suggested that the selection of 4P^r strains should yield an enriched population of mutants lacking AA-CoA transferase activity, due to a mutation in either the gene(s) encoding AA-CoA transferase or the putative activator locus, *atoC*.

Strains containing mutations in the genes encoding either AA-CoA transferase or the putative *ato* activator (*atoC*) were generated by plating the *atoC*(Con) constitutive mutant strain LS5218 onto solid medium supplemented with decanoate and 4P. The resulting 4P^r colonies, isolated at a frequency of 10^{-6}, were screened for their ability to grow on either AA or BUT. When the 4P^r colonies were screened for growth on AA and BUT as a sole carbon source, 90% were AA$^-$ But$^-$ and 10% were AA$^+$ But$^-$. The AA$^+$ But$^-$ isolates were presumed to be *atoC*$^+$ revertants of *atoC*(Con) and were not further characterized. The mutations resulting in the AA$^-$ 4P^r phenotype in 10 independent isolates were localized to the *ato* region by transduction with phage φP1 *vir* grown on strain LJ7 (*zeh-7*::Tn*10*) (data not shown).

Biochemical analysis of the AA$^-$ 4P^r isolates revealed that two mutants, designated strains LJ14 and LJ32, lacked AA-CoA transferase activity but maintained constitutive levels of thiolase activity (Table 3). Strain LJ32 failed to revert to AA$^+$, whereas strain LJ14 reverted to AA$^+$ at a frequency of 10^{-6}. These two isolates were presumed to harbor mutations in the locus (or loci) that encodes AA-CoA

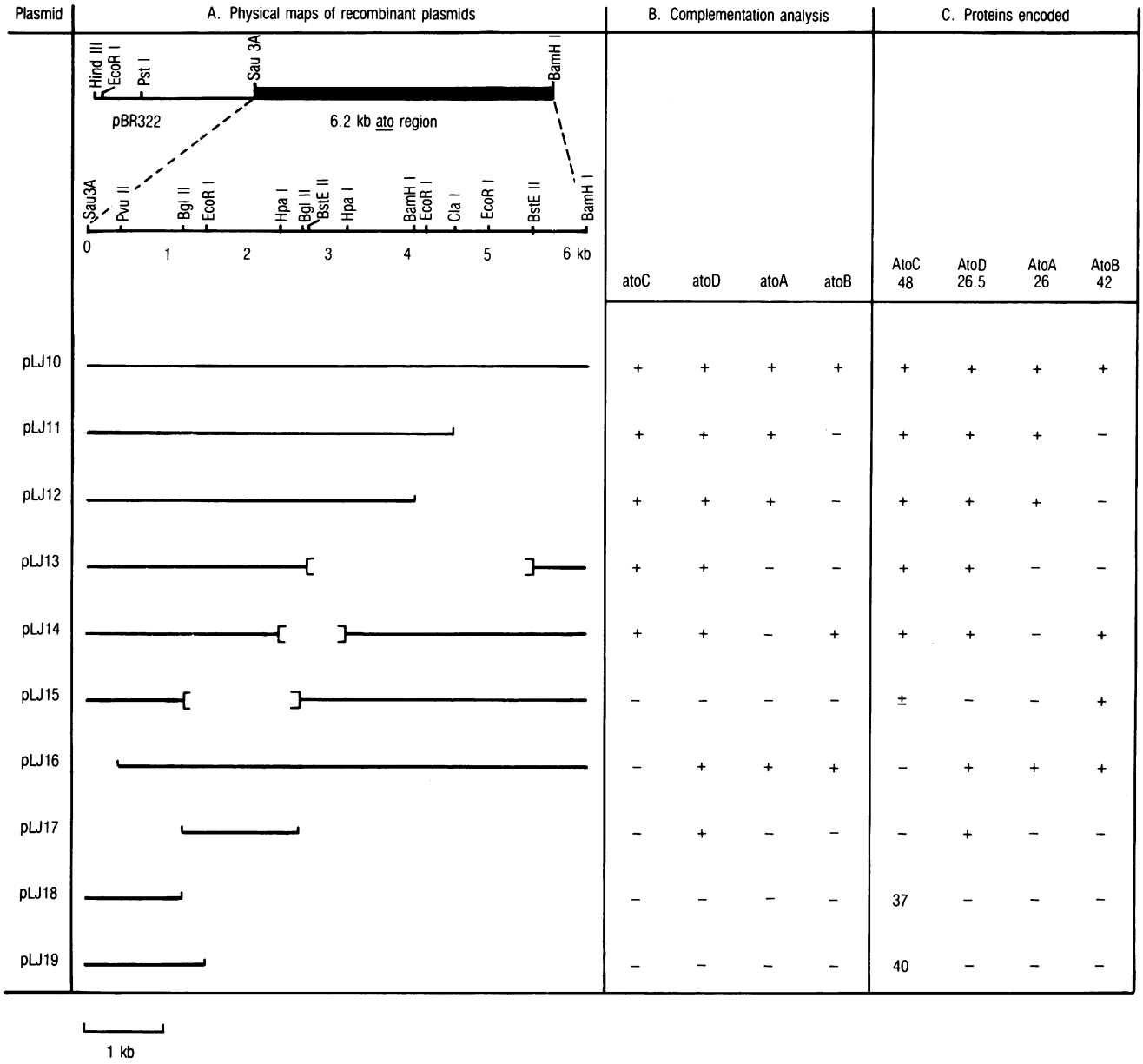

FIG. 2. Physical maps, complementation patterns, and protein profiles of the *atoCDAB* clone and subclones. (A) Physical maps of the *ato* clone and subclones. (B) Complementation pattern of the *ato* clone and subclones in the following *ato* hosts: *atoC*, LJ31 and LJ61; *atoD*, LJ32; *atoA*, LJ14 and K2006; *atoB*, K2009. Symbols: +, growth on 10 mM AA within 2 to 3 days; −, no growth. (C) Protein profiles of the *ato* clones and subclones derived from Fig. 3 and 4. Sizes are shown as 10^3 M_r.

transferase, with strain LJ32 carrying a deletion, insertion, or rearrangement and strain LJ14 having a point mutation in the *atoA* region. Two AA^- $4P^r$ isolates lacking both AA-CoA transferase and thiolase enzyme activities were classified as putative *atoC* mutants, designated strains LJ31 and LJ61 (Table 3). The low noninducible thiolase levels observed in these strains were due to constitutive levels of the *fadA*-encoded enzyme (thiolase I). Strain LJ31 reverted to AA^+ at a frequency of 10^{-6}, and strain LJ61 failed to revert to AA^+, suggesting that strain LJ31 contains a point mutation whereas strain LJ61 contains a deletion, insertion, or rearrangement in the *atoC* region.

Cloning of the *ato* genes from the *E. coli* chromosome. To obtain a recombinant plasmid that would contain the *atoCAB* gene complex, a partial *Sau*3A *E. coli* genomic library in pBR322 was used to transform an *atoA* mutant to ampicillin resistance. The Amp^r transformants were screened for their ability to grow on AA as a sole carbon and energy source. From a pool of 10,000 transformants, one AA^+ transformant was obtained. This AA^+ Amp^r transformant, designated pLJ10, contained a 10.5-kb recombinant plasmid and was further characterized and used throughout this study. Plasmid pLJ10 could transform independently isolated *ato* mutant strains to AA^+ Amp^r with a high efficiency (Fig. 2). It was therefore presumed to carry the *ato* structural genes and the putative regulatory gene, *atoC*. AA-CoA transferase and thiolase activities were measured in *ato* mutants harboring pLJ10. Both enzyme activities

TABLE 4. AA-CoA transferase and thiolase enzyme activities in *ato* mutant strains[a] containing various *ato* plasmids

Plasmid	Complementation by plasmid:				Sp act (nmol/min per mg of protein)[b]		
					AA-CoA transferase		Thiolase (K2009)
	atoC	*atoD*	*atoA*	*atoB*	LJ32	K2006	
pBR322	−	−	−	−	0	0	0
pLJ10	+	+	+	+	293	1,406	619
pLJ11	+	+	+	−	ND[c]	1,790	0
pLJ12	+	+	+	−	ND	1,613	0
pLJ13	+	+	−	−	41	0	0
pLJ14	+	+	−	+	21	0	803
pLJ15	−	−	−	−	0	0	17
pLJ16	−	+	+	+	ND	984	703
pLJ17	−	+	−	−	19	0	0
pLJ18	−	−	−	−	0	0	0
pLJ19	−	−	−	−	0	0	0

[a] Strains used for enzyme analysis were *recA* derivatives.
[b] A measurement of zero implies a specific activity of <0.1.
[c] ND, Not determined.

were restored when pLJ10 was present in the strains lacking either AA-CoA transferase activity (i.e., strains LJ32 and K2006) or thiolase activity (i.e., strain K2009) (Table 4).

To determine whether the *ato* genes on pLJ10 were regulated like the host chromosomal *ato*$^+$ genes, the ATO enzyme levels were measured in the Δ*ato* host, strain LJ112, containing this *ato* clone. When the Δ*ato* host was transformed with pLJ10, highly inducible ATO enzyme activities were observed (Table 5). These results suggested that the plasmid-encoded *ato* genes are regulated like the chromosomal *ato* genes. Therefore, the *atoC* gene on pLJ10 appears to be intact and the levels of the ATO enzymes do not appear to increase as a function of gene dosage.

Restriction map of pLJ10. Plasmid pLJ10 contains a 6.2-kb *E. coli* chromosomal DNA fragment, carrying the *ato* region, inserted into the *Bam*HI site of pBR322 (Fig. 2). The 6.2-kb insert contained a single restriction site for *Cla*I and *Pvu*II; two restriction sites each for *Ava*I, *Bam*HI, *Bgl*II, *Bst*EII, and *Hpa*I; three restriction sites for *Eco*RI; and at least four restriction sites each for *Eco*RV and *Hin*cII. There were no restriction sites for *Bal*I, *Kpn*I, *Sma*I, *Sst*I, *Sst*II, *Xba*I, or *Xho*I.

Subcloning the *ato* genes and complementation analysis. To develop a physical map of the *ato* region, various restriction endonuclease-generated fragments were deleted from pLJ10 (Fig. 2). The genotypes of the derivative plasmids were determined by complementation in strains defective in AA-CoA transferase activity (LJ32, LJ14, and K2006), defective in thiolase activity (K2009), defective in both AA-CoA transferase and thiolase activities (the *atoC* strains LJ31 and LJ61), and the Δ*ato* host LJ112 (Fig. 2). All complementation studies were performed in *recA* hosts.

The preliminary complementation pattern of these various subclones suggested that *atoB* was located in the 4.0- to 6.2-kb region and the gene(s) encoding the subunits of AA-CoA transferase was in the 1.0- to 4.0-kb region of the *ato* insert (Fig. 2). Strains defective in AA-CoA transferase activity (LJ32, LJ14, and K2006) had two complementation patterns (Table 4). When plasmids pLJ13 and pLJ14 were introduced into strain LJ32, AA-CoA transferase activity was restored, but when these plasmids were introduced into strains LJ14 and K2006, AA-CoA transferase activity was not restored. This finding suggested that two genes may exist, designated *atoD* and *atoA*, which encode the subunits of AA-CoA transferase, with strain LJ32 carrying a mutation in the *atoD* locus and strains LJ14 and K2006 harboring mutations in the *atoA* locus. The complementation studies also enabled us to position the *atoC* gene in the 0.0- to 2.0-kb region of this insert (see below). Therefore, the relative order of the *ato* genes in pLJ10 is *actoCDAB*, which is consistent with the genetic mapping data of Pauli and Overath (22) showing the order of the *ato* chromosomal genes as *atoCAB*.

To verify the complementation results, AA-CoA transferase and thiolase enzyme assays were performed in *atoD*, *atoA*, and *atoB* hosts harboring pLJ10 and the pLJ10 derivatives. The subclones that failed to complement the *atoA* mutation in strains K2006 and LJ14 also failed to restore AA-CoA transferase activity when introduced into the *atoA* mutant K2006 (Table 4). AA-CoA transferase activity was restored when pLJ13, pLJ14, and pLJ17 were introduced into the putative *atoD* host LJ32. The enzyme analysis therefore supports the previous complementation data indicating that two genes encode the subunits of AA-CoA transferase. The relatively low levels of AA-CoA transferase activity observed when pLJ13, pLJ14, and pLJ17 were introduced into the *atoD* mutant LJ32 may be due to the mixing of functional and nonfunctional subunits synthesized from both the host- and plasmid-encoded *atoA* and *atoD* genes.

Subclones which failed to complement the *atoB* mutation (pLJ11, pLJ12, and pLJ13) were unable to restore thiolase activity when introduced into the *atoB* mutant K2009. When the *atoCDA*$^+$ Δ*atoB* plasmid pLJ12 was introduced into the Δ*ato* host LJ112, AA-CoA transferase activity was highly inducible (Table 5). The inducible level of AA-CoA transfer-

TABLE 5. *ato*-encoded enzyme activities in the Δ(*atoCDAB*) strain LJ112 containing various *ato* plasmids

Strain or plasmid	*ato*$^+$ genotype	Induction[a]	Sp act (nmol/min per mg of protein)[b]	
			AA-CoA transferase	Thiolase
LE392	*atoCDAB*	−	0	0
		+	67	556
pBR322		+	0	0
pLJ10	*atoCDAB*	−	0	8
		+	73	573
pLJ12	*atoCDA*	−	0	ND[c]
		+	348	0
pLJ13	*atoCD*	−	0	ND
		+	0	0
pLJ14	*atoCDB*	−	ND	0
		+	0	161
pLJ15	*atoB*	−	ND	4
		+	0	10
pLJ16	*atoDAB*	+	0	0
PLJ17	*atoD*	+	0	0
pLJ18		+	0	0
pLJ19		+	0	0

[a] See Table 3, footnote *a*.
[b] A measurement of zero implies activity of <0.1.
[c] ND, Not determined.

ase activity in strain LJ112 (Δ*ato*) carrying pLJ12 was five times greater than that in the same strain carrying pLJ10. Although the exact mechanism of control is not evident from these studies, the latter findings suggest that the 4.0- to 6.2-kb region of the *ato* insert may encode a component(s) which negatively controls AA-CoA transferase activity.

As indicated above, plasmid pLJ15, which contains a deletion from 1.2 to 2.6 kb of pLJ10, failed to complement all *ato* mutants tested (Fig. 2). This deletion appears to extend through the *atoC* and *atoD* regions, accounting for its inability to complement the *atoC* and *atoD* mutants examined. Comparison of the deletions and *atoB* complementation patterns of pLJ14 and pLJ15 (Fig. 2) indicates that the deletion in pLJ15 does not extend into the *atoB* locus. Unlike plasmid pLJ14, which contains an internal deletion in the 2.4- to 3.2-kb region of the *ato* insert, pLJ15 did not complement *atoB*. Furthermore, when Δ*ato* strain LJ112 contained pLJ14, highly inducible levels of thiolase activity were observed, whereas when the same host strain harbored pLJ15, low levels of thiolase activity were observed (Table 5). These results suggested that removal of the 1.2- to 2.6-kb *ato* region altered the synthesis or activity of the *atoB* gene product. Given the location of the deletions in pLJ14 and pLJ15 with respect to the *atoB* coding region (4.0 to 6.2 kb), coupled with the complementation patterns of these plasmids with *ato* mutants (Fig. 2), one can infer that the promoter which controls the inducible expression of *atoB* must be deleted in pLJ15 and intact in pLJ14. Low levels of thiolase activity observed with pLJ15 may be due to a fortuitous promoter in pLJ10 upstream from the *atoB* promoter gene (e.g., the *atoC* promoter or a promoter within the vector, pBR322).

The mutation in strains LJ31 and LJ61 caused the simultaneous loss of AA-CoA transferase and thiolase activities (Table 3). This phenotype could be attributed to either a *cis*-dominant mutation which exerts a polar effect on the expression of the *ato* structural genes or a *trans*-recessive mutation which results in the loss of an activator required for the synthesis or activation of the *ato* structural gene products. Evidence supporting the latter alternative was obtained by the finding that the *atoCD*$^+$ Δ(*atoAB*) plasmid pLJ13 complemented strains LJ31 and LJ61 (Fig. 2). These results led us to conclude that the *trans*-recessive mutation in strains LJ31 and LJ61 may be in the *atoC* locus.

The approximate location of the *atoC* coding region on pLJ10 was obtained from complementation studies with the putative *atoC* mutant strains LJ31 and LJ61 and various subclones (Fig. 2). The complementation pattern of these subclones suggested that *atoC* was located in the 0.0- to 2.0-kb region of the *ato* insert. The *atoC* coding region must extend beyond the 1.5-kb region since a plasmid (pLJ19) containing the 0.0- to 1.5-kb region failed to complement strains LJ31 and LJ61.

Removal of the 0.0- to 0.5-kb region of pLJ10 resulted in a plasmid (designated pLJ16) that complemented *atoC*(Con) *atoD*, *atoC*(Con) *atoA*, and *atoC*(Con) *atoB* mutants but not *atoC* mutants (Fig. 2). The host-encoded *atoC*(Con) gene product appeared to act in *trans*, complementing the deleted *atoC* mutation in pLJ16. Not surprisingly, the subclone pLJ16 restored AA-CoA transferase and thiolase activities to *atoC*(Con) *atoD*, *atoC*(Con) *atoA*, and *atoC*(Con) *atoB* mutants (Table 4). However, this subclone did not restore AA-CoA transferase or thiolase activities to a Δ(*atoCDAB*) host strain (Table 5). These studies indicated that removal of the 0.0- to 0.5-kb region of pLJ10 did not exert a polar effect on the expression of the plasmid-encoded *atoD*, *atoA*, or *atoB* and the small 0.0- to 0.5-kb deletion resulted in the loss of a regulatory component (i.e., the AtoC activator) which is required for the synthesis or activation of the ATO enzymes.

Identification of the *atoCDAB* gene products. The maxicell procedure was initially used to identify the proteins encoded by pLJ10 and the pLJ10 derivatives. The coupled in vitro transcription-translation procedure was used and gave results similar to those of the maxicell protein profiles. The molecular weights of the plasmid-encoded proteins were identical in both labeling procedures.

pLJ10 encodes at least four unique polypeptides of molecular weights 48,000 (48K), 42K, 26.5K, and 26K (Fig. 3). To identify and distinguish the 26.5K protein from the slightly smaller 26K protein, the samples were analyzed by two-dimensional gel electrophoresis. In the maxicell procedure the 48K protein could barely be detected, whereas in the coupled in vitro transcription-translation procedure this protein was easily identifiable. Even in the in vitro system, the 48K protein appeared to be expressed at lower levels than the 42K, 26.5K, and 26K proteins. This may reflect the promoter strength of the gene that encodes the 48K protein, or auxiliary factors, limiting in this system, may be required for the expression of the gene which encodes the 48K protein.

Figure 2 summarizes the protein profiles observed in Fig. 3 and 4. Briefly, plasmids which were unable to complement the *atoB* defect or restore *atoB* enzyme activity to the *atoB* host resulted in the loss of the 42K protein, designated AtoB. Plasmids which complemented the *atoD* mutation in strain LJ32 but not the *atoA* mutation in strains K2006 and LJ14 expressed the 26.5K protein (designated AtoD) and lacked the 26K protein (designated AtoA). The plasmid pLJ16, which contained a deletion in the putative *atoC* gene, did not express the 48K protein, designated AtoC. Since both in vivo and in vitro protein analyses were performed in *atoC*$^+$ hosts, loss of AtoC in pLJ16 did not prevent the expression of the *ato* genes (Fig. 3f). A 37K and 40K protein were observed with pLJ18 ad pLJ19, respectively (Fig. 4). These subclones appear to encode truncated, nonfunctional AtoC polypeptides. These data also suggest that the direction of transcription of the *atoC* gene is from 0.0 to 1.5 kb.

Removal of the 1.2- to 2.6-kb region of the *ato* insert (i.e., pLJ15) resulted in the loss of the 26.5K and 26K proteins, while the 42K and 48K proteins were observed. The appearance of the 42K AtoB protein correlated with the low yet measurable levels of thiolase activity observed in pLJ15. The appearance of a 48K protein was a surprise, since (i) a plasmid containing the identical 0.0- to 1.2-kb *atoC* region (pLJ18) was found to encode a truncated AtoC polypeptide of 37K and (ii) plasmid pLJ19, containing the 0.0- to 1.5-kb *atoC* region, expressed a truncated 40K AtoC protein. Although a 48K protein was encoded by pLJ15, this plasmid was unable to complement the *atoC* mutations in strains LJ31 and LJ61. This indicates that pLJ15 does not encode a functional *atoC* gene product. A possible explanation for the appearance of a 48K protein encoded by pLJ15 is that the 1.2 to 2.6-kb deletion within the *ato* region generates a protein fusion that fortuitously results in a protein of 48K.

The protein profiles of pLJ10 and the various *ato* subclones supports the complementation studies and enzyme analyses, resulting in a detailed physical map of the 6.2-kb *ato* region, diagrammed in Fig. 5.

Polar insertion mutations within pLJ10. To determine the transcriptional arrangement of the *ato* structural and regulatory genes, polar mutations were generated within the 6.2-kb *ato* region by mutagenizing plasmid pLJ10 with a specialized

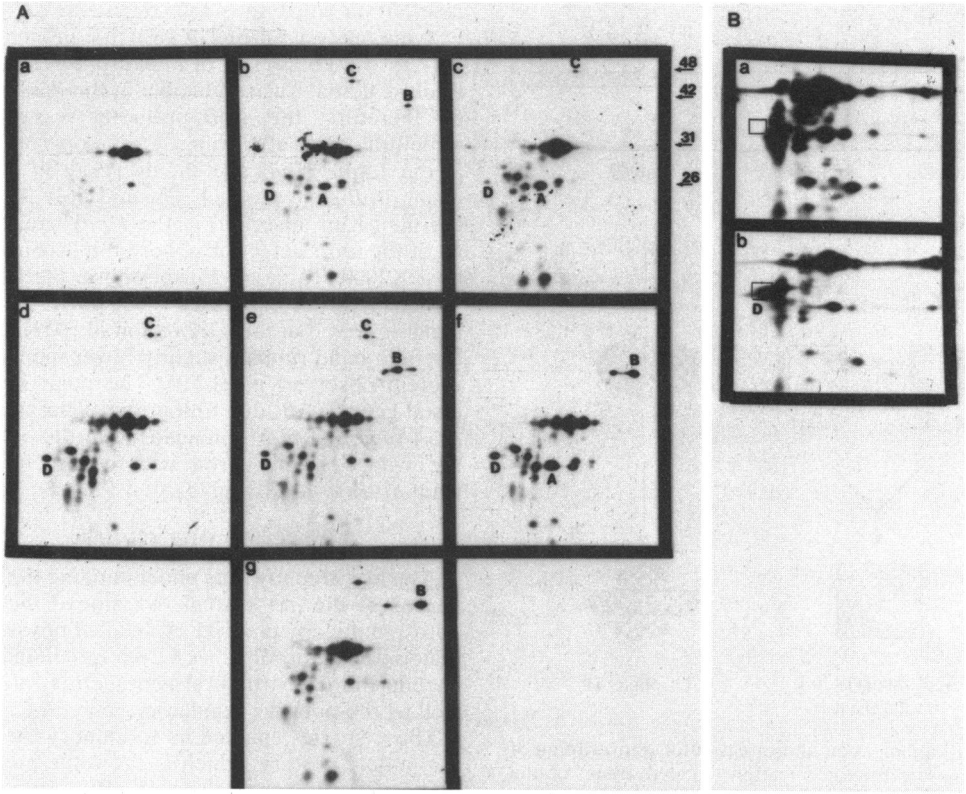

FIG. 3. Two-dimensional gel electrophoresis of [^{35}S]methionine-labeled plasmid-encoded proteins from the *atoCDAB* clone pLJ10 and various subclones. Labeled proteins were obtained by using a coupled in vitro transcription-translation procedure. (A) Panels: a, pBR322; b, pLJ10; c, pLJ12; d, pLJ13; e, pLJ14; f, pLJ16; g, pLJ15. C, B, D, and A indicate positions of the AtoC, AtoB, AtoD, and AtoA proteins, respectively. Sizes (10^3 M_r) are indicated. (B) Panels: a, pK09; b, pLJ17. D indicates the position of the AtoD protein. pH gradient is from 4.1 (left) to 8.9 (right); 12% polyacrylamide gels were used.

transposon, referred to as a mini-Kan^r element. This 1.67-kb mini-Kan^r element contains the gene that encodes Kan^r flanked by deleted IS*10* elements. Mutagenesis with the mini-Kan^r element can destroy gene function by (i) the insertional inactivation of a gene(s) or (ii) prevention of the expression of a gene(s) distal to the site of the insertion. Derivatives of pLJ10 carrying random mini-Kan^r insertions were screened for their ability to complement *atoC*, *atoD*, *atoA*, *atoB*, and Δ(*atoCDAB*) mutations within the host chromosome. All Km^r plasmids that resulted in an AA$^-$ phenotype in at least one of the *ato* mutant strains were further characterized. Figure 6 localizes the insertion site of the 1.67-kb mini-Kan^r element within pLJ10 and summarizes the complementation pattern of these plasmids.

Characterization of polar insertions within the *atoC* locus of pLJ10. The plasmids which contained a mini-Kan^r insertion at approximately 0.2, 1.0, and 1.6 kb of the *ato* insert (pMKC1, pMKC2, and pMKC3, respectively) were unable to complement the *atoC* mutations in LJ31 and LJ61 but could complement the *atoD* and *atoA* mutations in LJ32 and K2006, respectively, and the *atoB* mutation in K2009. When pMKC1, pMKC2, or pMKC3 was present in the *atoC* strains LJ31 and LJ61, the resulting transformants lacked both AA-CoA transferase and thiolase activities. But when these plasmids were introduced into the *atoC*(Con) *atoAB* host K2008, the *atoDAB*-encoded enzyme activities were restored (Table 6). The complementation data and enzyme analyses suggest that these mini-Kan^r insertions inactivated the *atoC*-encoded protein but did not interfere with the expression of the distal *atoD*, *atoA*, or *atoB* genes.

To correlate the loss of the *atoC*-encoded activator with the loss of or alteration in the 48K AtoC protein, the proteins of pMKC1, pMKC2, and pMKC3 were identified by the in vitro transcription-translation procedure. pMKC1 and

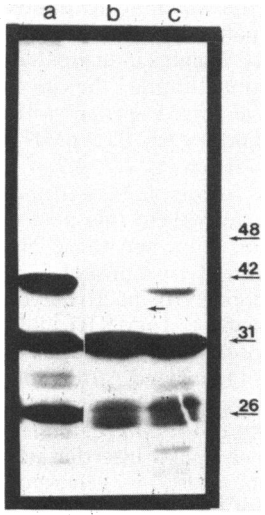

FIG. 4. One-dimensional gel electrophoresis of [^{35}S]methionine-labeled plasmid-encoded proteins from pLJ10, pLJ18, and pLJ19. Labeled proteins were obtained by using a coupled in vitro transcription-translation procedure. Lanes: a, pLJ10; b, pLJ18 (arrow indicates the plasmid-encoded protein); c, pLJ19. Proteins are indicated (10^3 M_r).

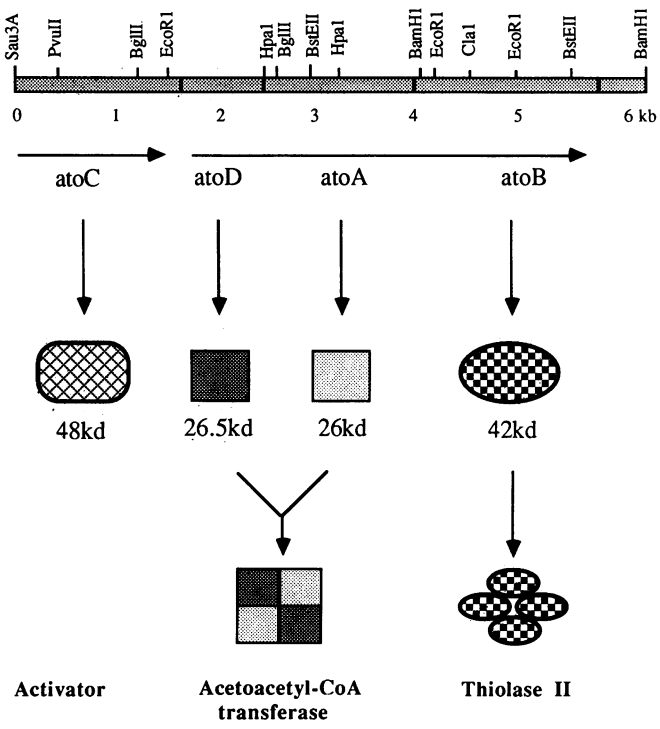

FIG. 5. Structural organization and direction of transcription of the *atoCDAB* genes. The relative location (shaded areas) of the *atoC*, *atoD*, *atoA*, and *atoB* genes and the direction of transcription are indicated. The endpoints of these genes are not precisely defined and are indicated by a vertical line. kd, 10^3 M_r.

pMKC2 resulted in the absence of the 48K protein, while pMKC3 resulted in low yet detectable level of the 48K protein (Fig. 7). Since pMKC3 resulted in a lack of the *atoC* activity, the presence of the 48K protein may be the due to the polar insertion occurring very close to the 3'-terminal end of the *atoC* gene. This could result in deletion of a few essential amino acids which may cause the loss of *atoC* activity but leave the M_r of AtoC almost unchanged. The complementation pattern, enzyme analyses, and protein profiles of the pMKC isolates indicate that *atoC* is not part of the same transcriptional unit as the *ato* structural genes.

Characterization of polar insertions within the *atoB* locus of pLJ10. The plasmids pMKB1, pMKB2, pMKB3, and pMKB4 contain insertions at 4.2, 4.7, 5.2 and 5.5 kb of the *ato* insert and failed to complement the *atoB* defect in K2009 or restore thiolase activity to this host (Table 6). Complementation was observed when these plasmids were introduced into the *atoD* and *atoA* hosts LJ32, LJ14, and K2006. These insertions appear to inactivate only the *atoB* gene product. Protein profiles of pMKB1 and pMKB2 showed a lack of the 42K AtoB gene product, whereas pMKB3 and pMKB4 expressed a truncated AtoB protein of 40K (Fig. 7). These data suggest that the direction of transcription of *atoB* is from 4.0 to 5.5 kb of the *ato* region.

Characterization of a polar insertion within the *atoA* region of pLJ10. Mini-Kan^r insertions, generated in vivo, were not scattered throughout the *ato* region. Independently isolated AA$^-$ Km^r plasmids were found to carry insertions in identical sites, and insertions were not obtained in vivo between 1.6 and 4.2 kb of the *ato* region. To insert a polar mutation between the putative promoter within the 1.2- to 2.6-kb region and the *atoB* gene, the 1.67-kb mini-Kan^r element was inserted in vitro into the *Hpa*I site of pLJ14. Previous enzyme analysis of pLJ14 (which contains a deletion in the 2.4- to 3.2-kb region of the *ato* insert) had shown that thiolase activity was inducible in the presence of AA (Table 5); therefore, the *atoB* promoter was intact. If the *ato* structural genes are arranged as an operon, a polar mutation at the 2.4-kb *Hpa*I site should result in inactivation of the distal *atoB* gene product. Plasmid pMKA, which contained the mini-Kan^r insertion in the *Hpa*I site, failed to complement the *atoB* defect or restore thiolase activity to the *atoB* host K2009 (Table 6). Furthermore, the 42K *atoB*-encoded protein was not expressed from pMKA (Fig. 7). The faint band observed at the 42K region of pMKA corresponded to the faint band running slightly lower than the *atoB*-encoded protein observed in pLJ10. The polar inactivation of the distal gene, *atoB*, due to the mini-Kan^r insertion within the *atoA* region of pLJ10 indicates that the *ato* structural genes are arranged as an operon, with the direction of transcription from *atoD* to *atoB* (Fig. 5).

DISCUSSION

As a first step towards understanding the regulatory mechanisms of the *ato* system, we cloned the *atoCDAB* genes onto a multicopy plasmid. A detailed physical map of the *ato* region was determined. A 6.2-kb *E. coli* insert was shown to encode the *ato* structural genes *atoD*, *atoA*, and *atoB*, as well as the putative regulatory gene *atoC*.

These studies enabled us to identify the *atoB* gene product, a 42K protein, which is the same molecular weight as that reported for thiolase II (10). Two distinct thiolase enzymes are present in *E. coli*. Thiolase I, a 42K protein encoded by *fadA* (23, 29), has broad-range fatty acid specificity, whereas thiolase II has specificity for SCFAs (10, 22). Thiolase II cannot substitute for thiolase I since *fadA* mutants cannot be complemented by plasmids which encode functional thiolase II (L. Jenkins, unpublished observations).

Earlier studies by Frerman and co-workers had shown that AA-CoA transferase was composed of two nonidentical subunits of apparent M_r 23K and 26K (30). These subunits are similar to the 26K and 26.5K proteins encoded by pLJ10. Both the *atoD* region, which encodes the 26.5K protein, and the *atoA* region, which encodes the 26K protein, are required for AA-CoA transferase activity. These results suggest that the 26.5K and 26K polypeptides correspond to the α and β subunits, respectively, of AA-CoA transferase.

TABLE 6. ATO enzyme activities of the pMKC, pMKB, and pMKA plasmids in various backgrounds

Plasmid[a]	Host (genotype)	Induction[b]	Sp act (nmol/min per mg of protein)	
			AA-CoA transferase	Thiolase
pMKC[c]	LJ112 (Δ*atoCDAB*)	+	0	0
pMKC[c]	LJ61 (*atoC atoDAB*$^+$)	+	0	11
pMKC[c]	K2008 *atoC*(Con)*AB*	−	946	822
pMKB[d]	LJ112 (Δ*atoCDAB*)	+	256	0
pMKA	LJ112 (Δ*atoCDAB*)	+	0	0
pLJ14	LJ112 (Δ*atoCDAB*)	+	0	161

[a] See Fig. 6 for localization of the mini-kan insertion within the 6.2kb *ato* region of pLJ10.

[b] See Table 3, footnote *a*.

[c] Values reflect the average specific activities of pMKC1, pMKC2, and pMKC3 in each host.

[d] Values reflect the average specific activities of pMKB1, pMKB2, pMKB3, and pMKB4 in host LJ112.

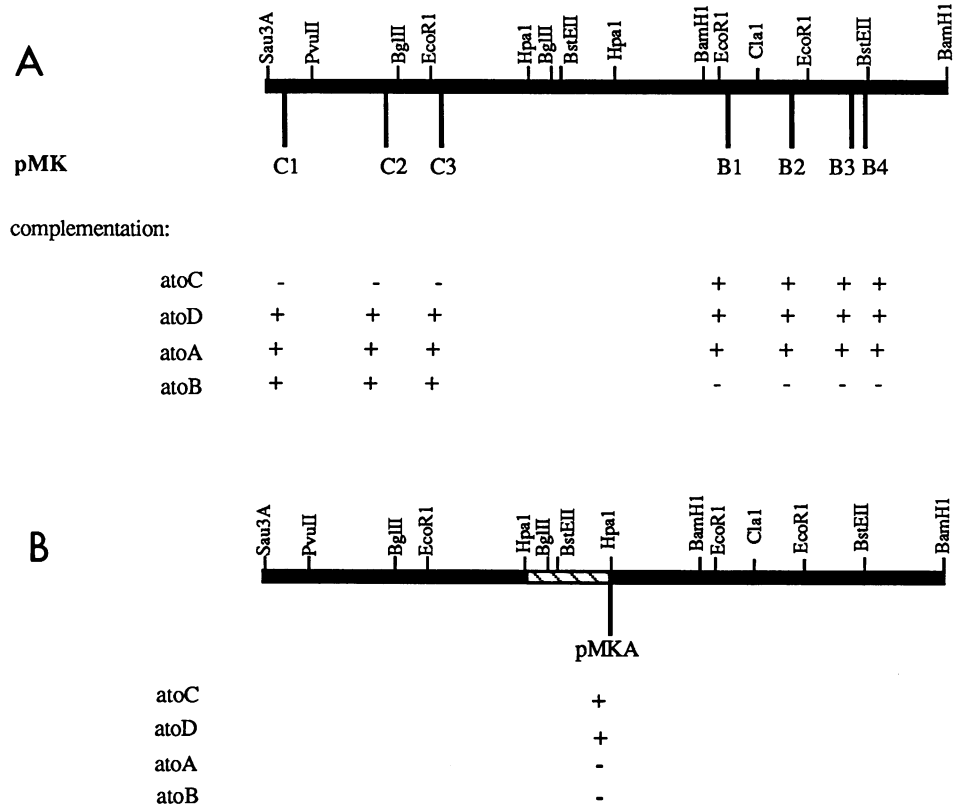

FIG. 6. Mini-Kan^r insertion map. (A) Mini-Kan^r insertion sites within the *atoC* and *atoB* regions of plasmid pLJ10. Complementation properties of the plasmids carrying mini-Kan^r insertions are presented below the insertion site. The following strains were used for complementation analyses: *atoC*, LJ31 and LJ61; *atoD*, LJ32; *atoA*, LJ14 and K2006; *atoB*, K2009. (B) Mini-Kan^r insertion in plasmid pLJ14, generated in vitro. The diagonal area represents the 2.4- to 3.2-kb deletion within the 6.2-kb *ato* insert.

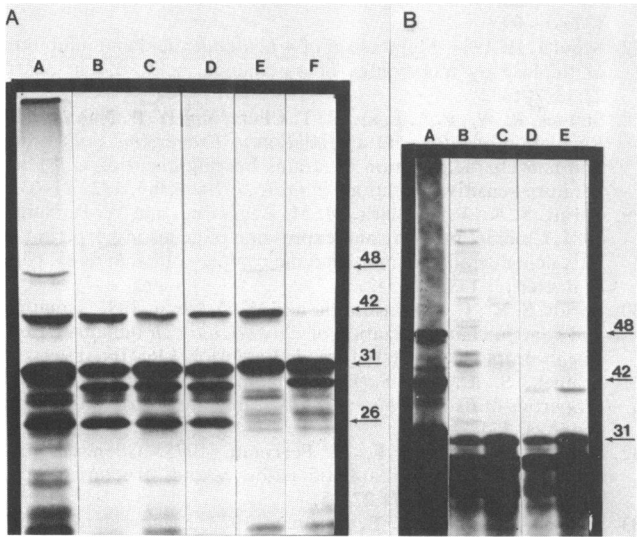

FIG. 7. Autoradiograms of [^{35}S]methionine-labeled plasmid-encoded proteins from plasmids with mini-Kan^r insertions in the 6.2-kb *ato* region. (A) Labeled proteins were obtained by using the coupled in vitro transcription-translation procedure and displayed on 12% polyacrylamide gels. Lanes: A, pLJ10; B, pMKC1; C, pMKC2; D, pMKC3; E, pLJ14; F, pMKA. (B) Labeled proteins were obtained by maxicell analysis and displayed on 9% polyacrylamide gels. Lanes: A, pLJ10; B, pMKB1; C, pMKB2; D, pMKB3; E, pMKB4. Proteins are indicated (10^3 M_r).

However, further studies showing that antibodies to the two subunits of AA-CoA transferase cross-react with the 26K and 26.5K proteins must be performed to confirm this hypothesis.

This work supports the suggestion of Pauli and Overath (22) that the *ato* structural genes form an operon. A polar insertion in the *atoA* gene resulted in the loss of the *atoB*-encoded thiolase activity and the 42K protein. A mini-Kan^r insertion in the *atoB* locus, however, resulted in the loss of only the *atoB* gene product and thiolase activity and had no effect on the adjacent *atoA* gene product. The fact that a single polar insertion in the *atoA* locus prevented the expression of the distal *atoB* gene product suggests that *atoA* and *atoB* are transcribed as a single transcriptional unit from *atoA* to *atoB*.

A 48K protein appears to be the *atoC* gene product. Several observations suggest that this protein is required for the synthesis or activation of the ATO enzymes: (i) *atoC* mutants were noninducible for these enzymes, (ii) plasmids containing deletions or insertions in *atoC* did not express the 48K protein or complement *atoC* mutants, (iii) plasmids containing deletions or insertions in the *atoC* locus expressed their *ato*-encoded enzymes in *atoC*(Con) *atoD*, *atoC*(Con) *atoA*, or *atoC*(Con) *atoB* host strains but not in *atoC* host strains, and (iv) an *atoC*$^+$ Δ*atoAB* plasmid, pLJ13, complemented *atoC* mutants.

Identification of the proteins encoded by the *atoC* subclones pLJ18 and pLJ19 revealed polypeptides of 37K and 40K, respectively. These plasmids appeared to encode nonfunctional, truncated AtoC proteins. The data also sug-

gest that the direction of transcription of the *atoC* gene is from 0.0 to 1.5 kb (Fig. 5), the same direction as the *atoDAB* operon. Polar insertions within the *atoC* locus resulted in simultaneous loss of the *atoDAB*-encoded enzyme activities. Since these enzyme activities were restored when the *atoC*(Con) allele was placed in *trans*, the polar insertion did not appear to interfere with the expression of the distal *atoDAB* genes. Therefore, the *atoC* locus is not part of the operon it controls.

This preliminary characterization of the *ato* region has revealed that the *ato* structural genes are arranged as an operon and have substantiated Pauli and Overath's contention (22) that the *atoC*-encoded protein functions as an activator. In an accompanying paper we will describe the regulatory mechanism by which the *atoC* gene product exerts control over the *ato* operon.

ACKNOWLEDGMENTS

We are grateful to Paul N. Black, Concetta DiRusso, and Kathleen Postle for many helpful discussions and technical advice. We especially thank Rowland Davis and the reviewers for the *Journal of Bacteriology* for critical reading of the manuscript. We thank Concetta DiRusso for generously providing the pBR322-*E. coli* library and Nancy Kleckner for providing phage λNK1105. We gratefully acknowledge the excellent technical assistance of Brad Hoo and Bryan Leigh. We also thank Esther Ervin for the figure illustrations.

The work was supported by Public Health Service grant GM-22466 from the National Institutes of Health. L.S.J. was supported by Public Health Services predoctoral fellowship GM-07311 from the National Institutes of Health.

LITERATURE CITED

1. **Adams, C. W., and G. W. Hatfield.** 1984. Effects of promoter strengths and growth conditions on copy number of transcription-fusion vectors. J. Biol. Chem. **259**:7399–7403.
2. **Adler, K., K. Beyreuther, E. Fanning, N. Giesler, B. Gronenborn, A. Klemm, B. Muller-Hill, M. Pfahl, and A. Schmitz.** 1972. How *lac* repressor binds to DNA. Nature (London) **237**:322–327.
3. **Bachman, B. J., and K. B. Low.** 1980. Linkage map of *Escherichia coli* K-12, edition 6. Microbiol. Rev. **44**:1–56.
4. **Berman, M. L., L. W. Enquist, and T. J. Silhavy.** 1981. Advanced bacterial genetics. Cold Spring Harbor Laboratory, Cold Spring Harbor, N.Y.
5. **Black, P. N., S. F. Kianian, C. C. DiRusso, and W. D. Nunn.** 1985. Long-chain fatty acid transport in *Escherichia coli*. Cloning, mapping, and expression of the *fadL* gene. J. Biol. Chem. **260**:1780–1789.
6. **Bolivar, F., R. L. Rodriguez, P. J. Greene, M. C. Betlack, H. L. Heynecker, and H. W. Boyer.** 1977. Construction and characterization of new cloning vehicles. II. A multipurpose cloning system. Gene **2**:95–113.
7. **Califano, L., and F. Villano.** 1947. Acido adenosintrifosforeco ed ossidazione dell'acido acetacetico nel bacterium coli. Boll. Soc. Ital. Biol. Sper. **23**:290–292.
8. **Dagert, M., and S. D. Ehrlich.** 1979. Prolonged incubation in calcium chloride improves the competence of *Escherichia coli* cells. Gene **6**:23–38.
9. **DiRusso, C. C., and W. D. Nunn.** 1985. Cloning and characterization of a gene (*fadR*) involved in regulation of fatty acid metabolism in *Escherchia coli*. J. Bacteriol. **161**:583–588.
10. **Duncombe, G. R., and F. E. Frerman.** 1976. Molecular and catalytic properties of the acetoacetyl-CoA thiolase of *Escherichia coli* Arch. Biochem. Biophys. **176**:159–170.
11. **Fong, J. C., and H. Schultz.** 1978. On the rate-determining step of fatty acid oxidation in heart. Inhibition of fatty acid oxidation in heart. Inhibition of fatty acid oxidation by 4-pentenoic acid. J. Biol. Chem. **253**:6917–6922.
12. **Helling, R. B., H. M. Goodman, and H. W. Boyer.** 1974. Analysis of endonuclease R *Eco*RI fragments of DNA from lamboid bacteriophages and other viruses by agarose gel electrophoresis. J. Virol. **14**:1235–1244.
13. **Humphreys, G. O., G. A. Willshaw, and E. S. Anderson.** 1975. A simple method for the preparation of large quantities of pure plasmid DNA. Biochim. Biophys. Acta **383**:457–463.
14. **Ish-Horowicz, D., and J. F. Burke.** 1981. Rapid and efficient cosmid cloning. Nucleic Acids Res. **9**:2989–2998.
15. **Kleckner, N., J. Roth, and D. Botstein.** 1977. Genetic engineering *in vivo* using translocatable drug-resistance elements. J. Mol. Biol. **116**:125–129.
16. **Lenti, C.** 1947. Sull'ossidazione dell'acido acetilacetico nell'Escherichia coli. Boll. Soc. Ital. Biol. Sper. **23**:296–297.
17. **Lowry, O. H., N. J. Rosebrough, A. L. Farr, and R. J. Randall.** 1951. Protein measurement with the Folin phenol reagent. J. Biol. Chem. **193**:265–275.
18. **Maloy, S. R., and W. D. Nunn.** 1981. Selection for the loss of tetracycline resistance by *Escherichia coli*. J. Bacteriol. **145**:1110–1112.
19. **Maniatis, T., E. F. Fritsch, and J. Sambrook.** 1982. Molecular cloning: a laboratory manual. Cold Spring Harbor Laboratory, Cold Spring Harbor, N.Y.
20. **Miller, J. H.** 1972. Experiments in molecular genetics. Cold Spring Harbor Laboratory, Cold Spring Harbor, N.Y.
21. **O'Farrell, P. H.** 1975. High-resolution two-dimensional electrophoresis of proteins. J. Biol. Chem. **250**:4007–4021.
22. **Pauli, G., and P. Overath.** 1972. *ato* operon: a highly inducible system for acetoacetate and butyrate degradation in *Escherichia coli*. Eur. J. Biochem. **29**:553–562.
23. **Pawar, S., and H. Schultz.** 1981. The structure of the multienzyme complex of fatty acid oxidation from *Escherichia coli*. J. Biol. Chem. **256**:3894–3899.
24. **Radloff, R., W. Bauer, and J. Vinograd.** 1967. A dye-bouyant-density method for the detection and isolation of closed circular duplex DNA: the closed circular DNA in HeLa cells. Proc. Natl. Acad. Sci. USA **57**:1514–1525.
25. **Salanitro, J., and W. Wegener.** 1971. Growth of *Escherichia coli* on short-chain fatty acids: growth characteristics of mutants. J. Bacteriol. **108**:893–901.
26. **Sancar, A., A. M. Hack, and W. D. Rupp.** 1979. Simple method for identification of plasmid-coded proteins. J. Bacteriol. **137**:692–693.
27. **Schultz, H.** 1983. Metabolism of 4-pentenoic acid and inhibition of thiolase by metabolites of 4-pentenoic acid. Biochemistry **22**:1827–1832.
28. **Simons, R. W., P. A. Egan, H. T. Chute, and W. D. Nunn.** 1980. Regulation of fatty acid degradation in *Escherichia coli*: isolation and characterization of strains bearing insertion and temperature-sensitive mutations in *fadR*. J. Bacteriol. **142**:621–632.
29. **Spratt, S. K., P. N. Black, M. M. Ragazzino, and W. D. Nunn.** 1984. Cloning, mapping and expression of genes involved in the fatty acid degradative multienzyme complex of *Escherichia coli*. J. Bacteriol. **158**:535–542.
30. **Spratt, S. K., C. L. Ginsburgh, and W. D. Nunn.** 1981. Isolation and genetic characterization of *Escherichia coli* mutants defective in propionate metabolism. J. Bacteriol. **146**:1166–1169.
31. **Sramek, S. J., and F. E. Frerman.** 1975. Purification and properties of *Escherichia coli* CoA-transferase. Arch. Biochem. Biophys. **171**:14–26.
32. **Sramek, S. J., and F. E. Frerman.** 1975. Coenzyme A-transferase: kinetics, catalytic pathway and structure. Arch. Biochem. Biophys. **171**:27–35.
33. **Sramek, S. J., and F. E. Frerman.** 1977. Steady state kinetic mechanism of the *Escherichia coli* coenzyme A transferase. Arch. Biochem. Biophys. **181**:178–184.
34. **Sramek, S. J., F. E. Frerman, and M. B. Adams.** 1977. Sulfhydryl group reactivity in the *Escherichia coli* CoA transferase. Arch. Biochem. Biophys. **181**:516–524.
35. **Way, J. C., M. A. Davis, D. Morisato, D. E. Roberts, and N. Kleckner.** 1985. New Tn*10* derivatives for transposon mutagenesis and for construction of *lacZ* operon fusions by transposition. Gene **32**:369–379.